PROCEEDINGS OF SCIENCE

Possible solution to the α-potential mystery in the γ-process and the Nd/Sm ratio in meteorites

T. Rauscher[*ab†]
[a] *Department of Physics, University of Basel, 4056 Basel, Switzerland*
[b] *Institute of Nuclear Research (ATOMKI), H-4001 Debrecen, POB 51, Hungary*
E-mail: Thomas.Rauscher@unibas.ch

The ^{146}Sm/^{144}Sm ratio in the early solar system has been constrained by Nd/Sm isotope ratios in meteoritic material. Predictions of ^{146}Sm and ^{144}Sm production in the γ-process in massive stars are at odds with these constraints and this is partly due to deficiences in the prediction of the reaction rates involved. The production ratio depends almost exclusively on the (γ,n)/(γ,α) branching at ^{148}Gd. A measurement of ^{144}Sm(α,γ)^{148}Gd at low energy had discovered considerable discrepancies between cross section predictions and the data. Although this reaction cross section mainly depends on the optical α+nucleus potential, no global optical potential has yet been found which can consistently describe the results of this and similar α-induced reactions. The untypically large deviation in ^{144}Sm(α,γ) can be explained, however, by low-energy Coulomb excitation which is competing with compound nucleus formation at very low energies. Low-energy (α,γ) and (α,n) data on other nuclei can also be consistently explained in this way. Since Coulomb excitation does not affect α-emission, the ^{148}Gd(γ,α) rate is much higher than previously assumed. This leads to very small ^{146}Sm/^{144}Sm stellar production ratios, in even more pronounced conflict with the meteorite data.

XII International Symposium on Nuclei in the Cosmos,
August 5-12, 2012
Cairns, Australia

[*] Speaker.

[†] Supported by the Hungarian Academy of Sciences, the European Commission within the FP7 ENSAR/THEXO project, and by the Collaborative Research Project MASCHE within the EuroGENESIS EuroCORE programme.

PoS(NIC XII)052

1. Introduction

The astrophysical γ-process synthesizes proton-rich nuclides through sequences of photodisintegrations of pre-existing seed material. It occurs in explosive Ne/O burning in core-collapse supernova (ccSN) explosions of massive stars [1, 2]. It is supposed to be the main source of the p-nuclides, i.e., naturally occurring, proton-rich nuclei which cannot be produced in the s- and r-process [3]. A recent investigation has shown that also type Ia supernovae (SNIa) may be a viable site for the γ-process [4], although previous simulations had not been successful [5, 6].

The γ-process produces both ^{146}Sm and ^{144}Sm, the production ratio $\mathscr{R} \equiv Y_{146}/Y_{144} = \lambda_{\gamma n}/\lambda_{\gamma\alpha} = R_{\gamma n}/R_{\gamma\alpha}$ depends on the stellar (γ,n) and (γ,α) rates of ^{148}Gd, denoted by $\lambda_{\gamma n}$ and $\lambda_{\gamma\alpha}$, respectively, or alternatively on the ratios of the reactivities, denoted by $R_{\gamma n}$ and $R_{\gamma\alpha}$ [7]. This ratio of particular interest because it was suggested that surviving ^{146}Sm may be detected in the solar system and used for cosmochronometry [8]. No live ^{146}Sm has been found to date but at least the signature of its in-situ decay in meteorites is believed to be seen, from which the isotope ratio at the closure of the solar system can be inferred [9, 10].

There are still large uncertainties involved in determining the production ratio, both from the side of astrophysical models and from nuclear physics. To better constrain the nuclear uncertainties ^{144}Sm(α,γ)^{148}Gd was measured in a pioneering, difficult experiment [11]. Since the stellar α-capture rate is dominated by the ground state (g.s.) transition [7, 12], the laboratory rate can be converted to the stellar (γ,α) rate by applying detailed balance [7,13]. Although the astrophysically relevant energy range of 9 MeV and below [14] could not be reached, the lowest datapoint at 10.2 MeV already showed a strong deviation from predictions. Using an optical α+nucleus potential with an energy-dependent part fitted to reproduce the data [11], a stellar (γ,α) rate was derived which was lower by an order of magnitude than previous estimates (see Table 1). This led to a strongly increased $\mathscr{R}$.

2. Optical α+nucleus potential and Coulomb barrier penetration

The findings of [11] have shed doubts on the predictions of (γ,α) rates at γ-process temperatures and triggered a number of experimental and theoretical studies. Due to the low cross sections, however, data is still scarce in the relevant mass region (at neutron numbers $N \geq 82$) and close to astrophysical energies. A comparison of predictions to data at higher energy often is irrelevant because the cross sections depend not just on the α-widths, as they do at low energy [12]. Many local and global optical α+nucleus potentials have been derived, using elastic scattering at higher energy, reaction cross sections, and theoretical considerations (like folding potentials). For examples, see, e.g., the list of potentials provided in [15]. None of the potentials are able to describe the existing (α,γ) and (α,n) data consistently, yet.

Two interesting observations can be made. Firstly, it was pointed out that the computation of barrier penetration factors far below the Coulomb barrier strongly depends on the assumed Coulomb radius of the potential (which often is not even specified in literature) and the numerical methods employed [13]. One has to be careful to choose a numerically stable treatment to determine Coulomb wave functions for low energy and high Coulomb barrier. Figure 1 compares two calculations making use of the same input but different routines for Coulomb transmission.

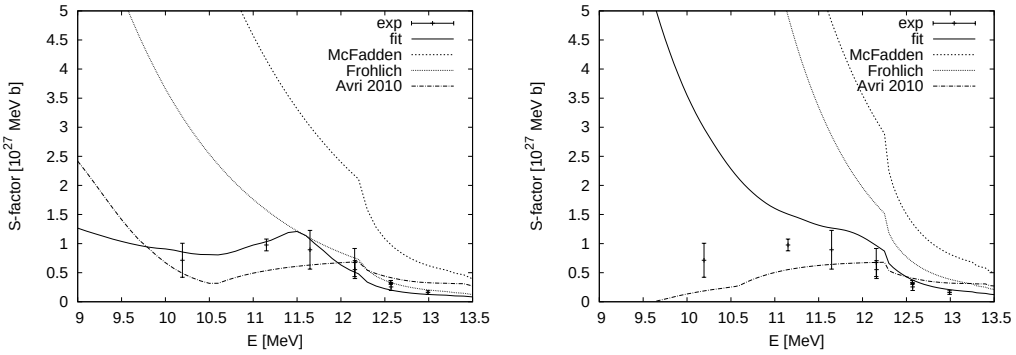

Figure 1: S-factors of ^{144}Sm(α,γ)^{148}Gd with the old routine [11, 18] for Coulomb transmission (left) and with the new routine [13,19] (right). The data (exp) [11] are compared to calculations obtained with different optical potentials, by [17] (McFadden), [20] (Frohlich), [21] (Avri 2010), and the fitted potential of [11].

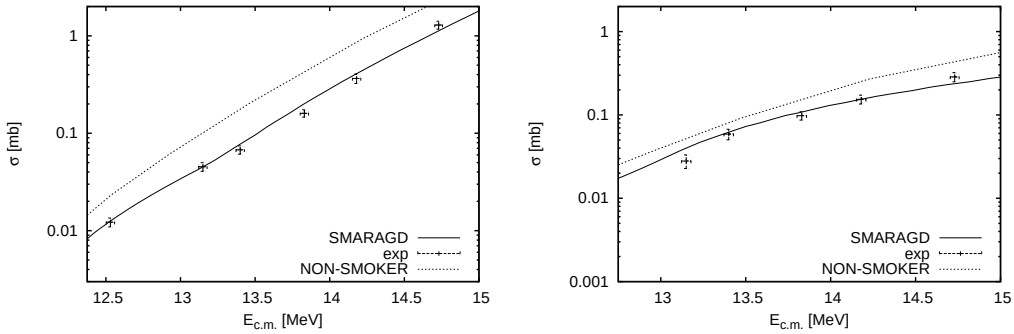

Figure 2: Cross sections of ^{168}Yb(α,n)^{171}Hf (left) and ^{168}Yb(α,γ)^{171}Hf (right); the experimental data [22] are compared to the predictions of NON-SMOKER [18] and SMARAGD [19], using their standard settings and the standard potential [17].

Secondly, using the modern, more accurate method to treat barrier penetration and using the standard potential of [17] (which was derived by fitting α-scattering data available at 24.7 MeV across a wide range of masses), a seemingly confusing picture arises. Some of the low-energy data are described well (an example is shown in Fig. 2, a similar one is ^{130,132}Ba(α,n) [16]), the majority of cases find deviations increasing with decreasing energies but never exceeding overprediction factors $2-3$, and then there is the ^{144}Sm(α,γ) case with its large deviation. Also the energy dependence of the ^{144}Sm(α,γ) data is peculiar and cannot be reproduced by any prediction (unless fitted to the data). The only common factor seems to be that the predictions using [17] are either close to the data or considerably higher.

3. Low-energy Coulomb excitation

The low-energy deviations and their variation from one nucleus to another may be explained by an additional reaction channel acting but not considered in the optical potential used in the calculations. A possibility is a direct inelastic channel (direct elastic scattering is included in the

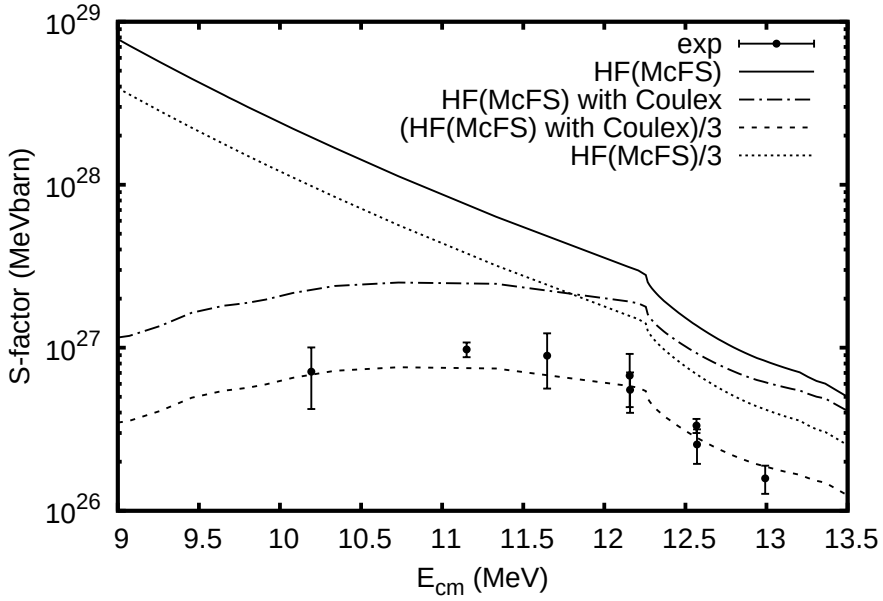

Figure 3: Experimental S-factors [11] (exp) for ^{144}Sm$(\alpha,\gamma)^{148}$Gd are compared to SMARAGD predictions using the standard potential [17] (McFS, full line), the same but corrected for Coulomb excitation (dash-dotted line), and the Coulex corrected prediction with the α-width divided by a constant factor of 3 (dashed line). Also shown is the standard prediction without correction but with the α-width divided by 3 (dotted line). The astrophysically relevant energy is about $8-9$ MeV [14].

usual optical potentials [23]). In the picture of the optical model, such a channel would divert part of the impinging α-flux away from the compound nucleus formation channel and thus lead to fewer compound nuclei at a given projectile flux. In the experiment this is seen as smaller reaction yield. Coulomb excitation (Coulex) is such a reaction mechanism and its importance at low energy in highly charged nuclei is plausible as it can be shown that for such nuclei the Coulex cross section $\sigma^{\rm Coulex}$ declines more slowly with decreasing energy than the compound formation cross section $\sigma^{\rm form}$, due to the Coulomb barrier.

The diversion of α-flux from the compound formation channel can be effectively accounted for by using a modified compound formation cross section (this can simply be implemented by using modified α-transmission coefficients in the *entrance* channel) $\sigma_\ell^{\rm form,mod} = f_\ell \sigma^{\rm form}$, with

$$f_\ell = \frac{\sigma_\ell^{\rm form}}{\sigma_\ell^{\rm form} + \sigma_\ell^{\rm Coulex}} \tag{3.1}$$

for each partial wave ℓ. The Coulex cross section can be calculated, e.g., by [24]

$$\sigma_\ell^{\rm Coulex} \propto B({\rm E}\mathscr{L}) \sum_{\ell_{\rm f}} \left\{ (2\ell_{\rm f}+1) \left| \int_0^\infty F_{\ell_{\rm f}}(k_{\rm f} r) r^{-\mathscr{L}-1} F_\ell(kr)\, dr \right| \right\} \quad , \tag{3.2}$$

using regular Coulomb wave functions $F_\ell(kr)$, $F_{\ell_{\rm f}}(k_{\rm f} r)$ at initial and final α-energies, respectively. The transition strengths for electric multipole emission of multipolarity $\mathscr{L}$ are given by $B({\rm E}\mathscr{L})$. The results shown here are for the dominant multipolarity $\mathscr{L}=2$, i.e., E2 transitions.

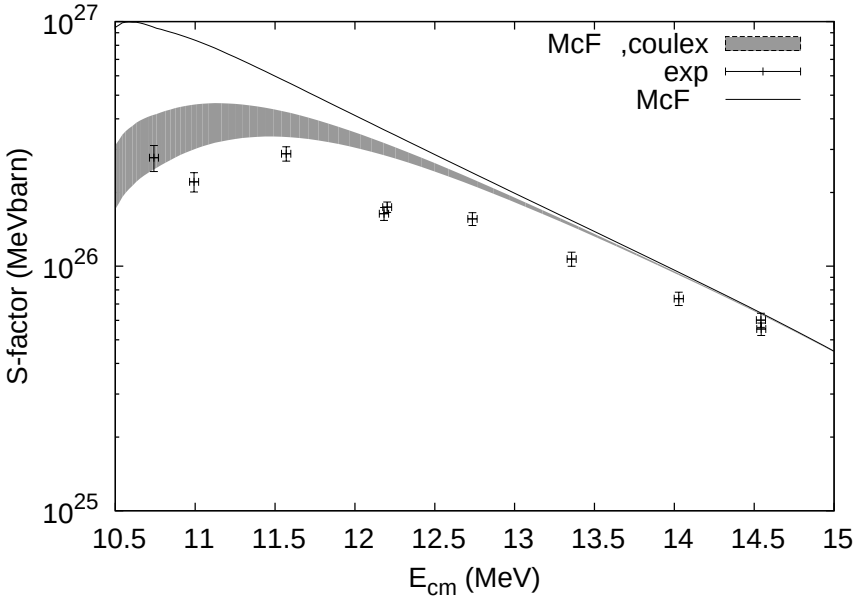

Figure 4: Experimental S-factors [25] (exp) for ^{141}Pr(α,n)^{144}Pm are compared to SMARAGD predictions using the standard potential [17] (McF) and correction for Coulomb excitation (McF, Coulex). The uncertainty introduced by the B(E2) values is shown by the shaded region. Note that the prediction including Coulex is only 20% above the data.

Figure 3 shows how the S-factor is changed by inclusion of Coulex while still using the standard potential (McFS [17]). The energy dependence of the data is now accurately reproduced but the absolute value is still too high. It was assumed in the calculation, however, that the optical potential used accurately describes compound formation in the absence of Coulex. This does not have to be the case, though, there may still be an additional energy dependence which has to be determined independently. The data can be perfectly described by renormalizing the α-widths obtained with the standard potential, as also shown in Fig. 3. The required factor of 1/3 is well in line with the typical deviations found for other α-induced reactions at low energy.

The approach outlined above should also remain valid when applied to other reactions. Due to the scarcity of suitable data, there are only few cases to be checked. As mentioned above, very good agreement was found between predictions and data for ^{130,132}Ba(α,n) [16]. Despite of the presence of low-lying 2^+ states, this remains so when including Coulex because the B(E2) values are very small and Coulex therefore negligible in the investigated energy range. Two other suitable cases are shown in Figs. 4 and 5, the reactions ^{141}Pr(α,n)^{144}Pm and ^{169}Tm(α,n)^{172}Lu, respectively. In both cases, the increasing deviation found for decreasing energy can be nicely explained by the acting of Coulex. A large uncertainty, however, remains in the B(E2) values which are experimentally not well determined for odd nuclei (or nuclei with g.s. other than 0^+). The prediction for ^{141}Pr(α,n) may need a small modification of the optical potential, it is 20% too high. But this is better still than the usually assumed uncertainties in astrophysical rate predictions. The large uncertainty stemming from the B(E2) value does not allow to draw a final conclusion on ^{169}Tm(α,n) but it seems that

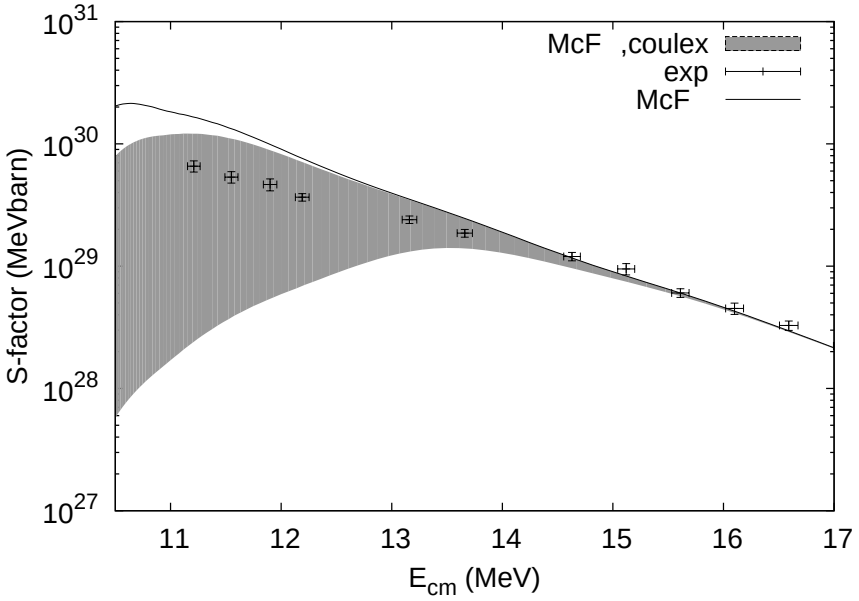

Figure 5: Experimental S-factors [26] (exp) for ^{169}Tm(α,n)^{172}Lu are compared to SMARAGD predictions using the standard potential [17] (McF) and correction for Coulomb excitation (McF, Coulex). The uncertainty introduced by the B(E2) values is shown by the shaded region.

it may be feasible to reproduce the energy dependence of the data without change in the optical potential.

4. Consequences

To assess the impact on the stellar ^{148}Gd(γ,α) rate it should be recalled that Coulex acts in the *entrance* channel but the α-emission channel should be unaffected. This is also the reason why an optical potential accounting for compound formation without including Coulex in its absorptive part has to be used. Only such a potential can then be applied to α-emission. (Detailed balance then applies to transitions obtained with such a potential.) This is not the potential that would be obtained by α-scattering. If it were possible to perform an α-scattering experiment at such low energy and extract an optical potential, this potential would include both compound formation and Coulex in its absorptive part but no information on how to distribute the flux across the two possibilities. Therefore it has to be realized that the result *without* Coulex has to be used for computing the stellar reactivity $N_{\rm A}\langle\sigma v\rangle^*$ for ^{144}Sm(α,γ), which then can be converted to the (γ,α) rate. Since the α-width had to be reduced to reproduce the data after Coulex was applied, it also has to be reduced in the original result without Coulex. This gives the dotted line shown in Fig. 3.

Table 1 compares the stellar reactivities for ^{144}Sm(α,γ) obtained with different codes (i.e., different treatment of Coulomb barrier penetration) and different potentials, as used in astrophysical applications. The final prediction is higher than all previous estimates (except the unrenormalized SMARAGD calculation with the standard potential) and in particular higher by two orders of magnitude than the value obtained by directly fitting the experimental results of [11]. This will lead to

Type	Code	Reactivity ($cm^3\ s^{-1}\ mole^{-1}$)	Ref.
Equivalent Square Well [27]	CRSEC	3.8×10^{-15}	[1]
Folding (real), Woods-Saxon (imag.)	SMOKER	1.3×10^{-15}	[28]
Woods-Saxon [17]	NON-SMOKER	1.9×10^{-15}	[18]
Woods-Saxon [17]	SMARAGD	2.4×10^{-14}	[19]
Energy-dep. Woods-Saxon [11]	MOST, SMOKER	1.3×10^{-16}	[11]
Energy-dep. Woods-Saxon [11]	SMARAGD	2.2×10^{-15}	[19]
Woods-Saxon [17], scaled α-width	SMARAGD	1.2×10^{-14}	this work

Table 1: Stellar ^{144}Sm(α,γ)^{148}Gd reactivities at 2.5 GK from different sources, obtained with different codes and different types of optical α+nucleus potentials. The codes SMOKER, NON-SMOKER, MOST used the same routine to calculate Coulomb barrier penetration.

a strongly reduced isotope ratio $\mathscr{R}$, which has to be determined in a full γ-process simulation. A simple estimate, however, can already be made. The new result is a factor of 3.2 higher than the value used in [1]. This is comparable to test case B in [7]. A production ratio $\mathscr{R} = 0.0064$ was estimated for case B [7]. This is well below the range of $0.1 \leq \mathscr{R} \leq 0.7$ suggested by the meteoritic data and allowing for a reasonable time for decay before solar system formation [7, 9, 11]. The original value of 0.015 obtained in [1] was also in conflict with the meteorite data. On the other hand, the much lower value found in [11] led to production ratios exceeding 0.7. To paraphrase Ref. [7], the very low value of $\mathscr{R}$ might "at least pose very interesting constraints upon chemical evolution and the formation of solids in the early solar system".

Further experiments may help to clarify the situation regarding the low-energy Coulex effect. The B(E2) values for odd nuclei have to be determined with higher precision. If possible, a simultaneous detection of the γ-emission from the excited target nucleus state while performing a reaction experiment could directly indicate the action of Coulex. Complementary measurements of α-absorption and -emission (not for ^{144}Sm, obviously, but for other test cases) should show a difference in the two directions, not accountable for by straightforward application of detailed balance. In this context it is interesting to note that (n,α) experiments on ^{143}Nd and ^{147}Sm find an overprediction by a factor of 3 [29–32]. This is fully consistent with the required renormalization found here, after correction for Coulex.

Question after talk at NIC: Do you expect any difference in Nd/Sm between SNIa and ccSN? Since both ^{146}Sm and ^{144}Sm originate from the photodisintegration of ^{148}Gd, their ratio does not depend on the seed. Not only the peak temperature reached in a zone, however, but also the temperature evolution, i.e., how much time is spent at a given temperature, impacts the final ratio. A higher temperature favors (γ,n) with respect to (γ,α) and increases ^{146}Sm production [7]. The Nd/Sm ratio thus also depends on the expansion timescale, higher explosion temperatures are relevant with shorter timescales. The expansion is different in different ccSN models and it may be very different for SNIa. Following the expansion of the expanding hot fragments of a SNIa – and thus of its actual nucleosynthesis – in detail requires accurate, high-resolution hydrodynamic modelling.

References

[1] S. E. Woosley and W. M. Howard, *Ap. J. Suppl.* **36** (1978) 285.

[2] T. Rauscher, A. Heger, R. D. Hoffman and S. E. Woosley, *Ap. J.* **576** (2002) 323.

[3] M. Arnould and S. Goriely, *Phys. Rep.* **384** (2003) 1.

[4] C. Travaglio, F. Röpke, R. Gallino and W. Hillebrandt, *Ap. J.* **739** (2011) 93.

[5] W. M. Howard, B. S. Meyer and S. E. Woosley, *Ap. J. Lett.* **373** (1991) L5.

[6] K. Nomoto, F.-K. Thielemann and K. Yokoi, *Ap. J.* **286** (1984) 644.

[7] S. E. Woosley and W. M. Howard, *Ap. J.* **354** (1990) L21.

[8] J. Audouze and D. N. Schramm, *Nature* **237** (1972) 447.

[9] A. Prinzhofer, D. A. Papanastassiou and G. A. Wasserburg, *Ap. J. Lett.* **34** (1989) L81.

[10] C. L. Harper, *Ap. J.* **466** (1996) 437.

[11] E. Somorjai *et al.*, *Astron. Astrophys.* **333** (1998) 1112.

[12] T. Rauscher, *Ap. J. Suppl.* **201** (2012) 26.

[13] T. Rauscher, *Int. J. Mod. Phys. E* **20** (2011) 1071.

[14] T. Rauscher, *Phys. Rev. C* **81** (2010) 045807.

[15] G. G. Kiss *et al.*, *Phys. Rev. C* **80** (2009) 045807.

[16] Z. Halász *et al.*, *Phys. Rev. C* **85** (2012) 025804.

[17] L. McFadden and G. R. Satchler, *Nucl. Phys.* **84** (1966) 177.

[18] T. Rauscher and F.-K. Thielemann, *At. Data Nucl. Data Tables* **79** (2001) 47.

[19] T. Rauscher, computer code SMARAGD, version 0.8.1s (2010).

[20] T. Rauscher, *Nucl. Phys.* **A719** (2003) 73.; *Nucl. Phys.* **A725** (2003) 295.

[21] M. Avrigeanu and V. Avrigeanu, *Phys. Rev. C* **82** (2010) 014606.

[22] A. Sauerwein, PhD thesis, University of Cologne, Germany (2012).

[23] G. R. Satcher, *Direct Nuclear Reactions*, Clarendon Press, Oxford 1983.

[24] K. Alder, A. Bohr, T. Huus, B. Mottelson and A Winther, *Rev. Mod. Phys.* **28** (1956) 432.

[25] A. Sauerwein *et al.*, *Phys. Rev. C* **84** (2011) 045808.

[26] T. Rauscher *et al.*, *Phys. Rev. C* **86** (2012) 015804.

[27] J. W. Truran, *Astrophys. Space Sci.* **18** (1972) 308.

[28] T. Rauscher, F.-K. Thielemann and H. Oberhummer, *Ap. J. Lett.* **451** (1995) L37.

[29] Yu. M. Gledenov *et al.*, *Phys. Rev. C* **62** (2000) 042801(R).

[30] P. E. Koehler *et al.*, *Nucl. Phys.* **A688** (2001) 86c.

[31] P. E. Koehler, Yu. M. Gledenov, T. Rauscher and C. Fröhlich, *Phys. Rev. C* **69** (2004) 015803.

[32] Yu. M. Gledenov Yu M *et al.*, *Phys. Rev. C* **80** (2009) 044602.